Silyl- and Germyl-Substituted Boranes: Synthesis and Investigation as Potential Atomic Layer Deposition Precursors

Majeda Al Hareri,[a] Patricio Romero,[b,c] James F. Britten,[d] David J. H. Emslie[a,*]

[a] Department of Chemistry, McMaster University, 1280 Main St. West, Hamilton, Ontario, L8S 4M1, Canada.

[b] Intel Corporation, Technology Research, 2511 NE Century Blvd., Hillsboro, OR 97124, USA.

[c] Current address: ASM, Corporate R&D, IMEC, Kapeldreef 75, Leuven, Belgium.

[d] McMaster Analytical X-Ray Diffraction Facility (MAX), McMaster University, 1280 Main St. West, Hamilton, Ontario, L8S 4L8, Canada.

Supporting Information Placeholder

ABSTRACT: Boranes featuring bulky hypersilyl or supersilyl groups, and/or sterically unencumbered trimethylgermyl substituents, were synthesized for investigation as potential precursors for ALD of elemental boron. The envisaged ALD process would employ a boron trihalide co-reactant, exploiting the formation of strong silicon-halogen and germanium-halogen bonds as a driving force. The alkali metal silyl and germyl compounds hypersilyl lithium, $\{(Me_3Si)_3Si\}Li(THF)_3$ (**1**), supersilyl sodium, $(^tBu_3Si)Na(THF)_n$ (**2**; n = 2-3), and trimethylgermyl lithium, $\{Me_3GeLi(THF)_2\}_2$ (**3**), were used for the synthesis of the silyl- and germyl-substituted boranes in this work. Compounds **1** and **2** were synthesized as previously reported, and compound **3** was isolated from the reaction of trimethylgermane with *tert*-butyl lithium. Compounds **2** and **3** were crystallographically characterized. Reaction of $B(NMe_2)Cl_2$ with two equiv. of **1** afforded previously reported $\{(Me_3Si)_3Si\}_2B(NMe_2)$ (**4**), whereas reactions of $B(NMe_2)Cl_2$ or $\{B(NMe_2)F_2\}_2$ with excess **2** only afforded the mono-silyl boranes $(^tBu_3Si)B(NMe_2)X$ {X = Cl (**5**) and F (**6**)}. Reaction of **5** with 0.5 equivalents of $\{Me_3GeLi(THF)_2\}_2$ (**3**) provided the first example of a mixed silyl/germyl-substituted borane, $(^tBu_3Si)(Me_3Ge)B(NMe_2)$ (**7**). Attempts to synthesize $(Me_3Ge)_2B(NMe_2)$ from the 1:1 reaction of $B(NMe_2)Cl_2$ with $\{Me_3GeLi(THF)_2\}_2$ afforded a mixture of two major products, one of which was identified as the tri(germyl)(amido)borate $\{(Me_3Ge)_3B(NMe_2)\}Li(THF)_2$ (**8**); compound **8** was isolated from the 1:1.5 reaction. Reaction of more sterically encumbered $B(TMP)Cl_2$ with one equivalent of $\{Me_3GeLi(THF)_2\}_2$ afforded the di(germyl)(amido)borane $(Me_3Ge)_2B(TMP)$ (**9**). Boranes **4**, **7** and **9**, and borate **8**, were crystallographically characterized. The thermal stability and volatility of boranes **4**, **7** and **9** was evaluated, the solution reactivity of **4** and **7** with boron trihalides was assessed, and ALD was attempted using **4** in combination with BCl_3 and BBr_3 at 150 and 300 °C.

INTRODUCTION

Ultra-thin films of elemental boron have a range of applications, including as barrier layers on silicon,[1] as layers in single-photon avalanche diodes for UV[2] and low-energy electron[3,4] detection, in neutron detectors,[5] and as etch-resistant films in micro-machining.[6,7] Furthermore, methods for elemental boron deposition have applications in doping of group 14 element-containing films (e.g. Si,[8] SiGe,[9,10] GeSn,[11,12] SiGeSn,[13] graphene,[14,15] diamond[16-18]) during microelectronic device or solar cell fabrication, and the synthesis of borophene (a 2D material composed of a crystalline monolayer of boron).[19,20] These applications typically employ chemical vapour deposition (CVD) or physical vapour deposition (PVD; e.g. evaporation, sputtering and molecular beam epitaxy) methods.[21] For CVD, highly toxic B_2H_6 is commonly used as the boron source, typically with deposition temperatures between 350 °C and 700 °C for plasma-free deposition.[22] Boron CVD using other precursors, such as BCl_3 in combination with H_2 at temperatures above 750 °C, has also been reported.[23]

Atomic layer deposition (ALD)[24] is an alternative deposition technique that can provide access to thin films that are more uniform and conformal than those accessible using other film growth methods. In addition, ALD is typically carried out at lower temperatures than those employed for CVD (e.g. 100-300 °C), making it compatible with a broader range of substrates. ALD relies upon self-limiting surface-based reactions between a precursor molecule and a co-reactant, which are delivered to the substrate surface in the vapour/gas phase, separated by inert gas purge steps. However, while ALD methods have been developed for several main group elements,[25] ALD of elemental boron has not yet been achieved.[26]

This work focuses on the synthesis of silyl- and germyl-substituted amidoboranes, $(R_3E)_2B(NR'_2)$ (E = Si or Ge), and investigation of their suitability as precursors, in combination with boron trihalides as co-reactants, for ALD of elemental boron. The general process envisaged for ALD of elemental boron is outlined in Scheme 1, and can be considered to involve (a) conversion of $(R_3E)_2B(NR'_2)$ to $(R_3E)_2BX$ (X = Cl or Br) via reaction with BX_3, generating $B(NR'_2)X_2$ as a volatile byproduct, and (b) reaction of $(R_3E)_2BX$ with BX_3 in a 3:1 ratio to afford 4 equivalents of elemental boron and 6 equivalents of R_3EX. Boron trichloride is commonly used to convert

amidoborane compounds to chloroboranes,[27-35] and analogous reactivity has also been reported with BBr_3,[36-40] so step (a) has ample precedent. Step (b) mirrors reactivity that has previously been used for ALD of elemental antimony ($Sb(SiR_3)_3 + SbCl_3 \rightarrow 2\ Sb(s) + 3\ R_3SiCl$; R = Me or Et), which relies upon the thermodynamically favourable formation of silicon-chlorine bonds as a driving force.[41,42] Analogous reactivity has also been reported for ALD of a range of binary materials, including ESb (E = Al or Ge),[42] E_2Se_3 (E = In or Bi),[43] Cu_2Se,[43] $MoSe_2$,[44] ETe (E = Ge or Zn),[43] and E_2Te_3 (E = Sb or Bi).[43,45] Furthermore, the silyldihaloboranes (^{t}Bu$_3$Si)BX_2 (X = Cl and Br) have been reported to eliminate ^{t}Bu$_3$SiX slowly at room temperature to afford unidentified boron subhalides.[46] Examples of R_3GeX elimination from a germyl-substituted haloborane have not been reported, to the best of our knowledge. However, thermal ALD processes involving germyl halide elimination have been developed. For example, Me_3GeCl was generated as a byproduct in $GeTe_2$ ALD utilizing $GeCl_4$ and $Te(GeMe_3)_2$.[47] Additionally, nickel and gold ALD relying upon Me_3GeCl elimination (in reactions of $[NiCl_2(PEt_3)_2]$[48] or $[AuCl(PEt_3)]$[49] with 1,4-bis(trimethylgermyl)-1,4-dihydropyrazine) has been described, and, in the case of nickel, was successful when analogous reactivity relying upon Me_3SiCl elimination was not. It is important to note that the envisaged chemistry (Scheme 1) requires two silyl/germyl groups in the borane precursor, and a similar scheme leading to elemental boron cannot be constructed for a mono(silyl/germyl)borane.

Scheme 1. Potential reactivity for boron ALD using $(R_3E)_2B(NR'_2)$ precursors (E = Si or Ge) in combination with a boron trihalide (BX_3; X = Cl or Br) co-reactant. (Note: surface-based reactivity will be more complex than that depicted in the scheme, which is meant to illustrate key reaction steps)

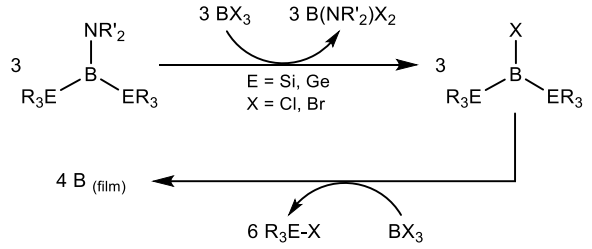

To be suitable for ALD, precursors must be sufficiently volatile, thermally stable, and reactive towards the desired co-reactant. Silyl-and germyl-substituted boranes bearing one dimethylamido group, $(R_3E)_2B(NR'_2)$ (E = Si or Ge), were targeted in this work, rather than tri(silyl/germyl)boranes, $B(ER_3)_3$, since they are expected to be more thermally robust as a result of electronic stabilization (π-donation from nitrogen to boron).[50,51] Silyl and germyl groups of differing steric bulk (extremely bulky Si^{t}Bu$_3$ and Si(SiMe$_3$)$_3$, and sterically unencumbered GeMe$_3$) were investigated in order to probe the effects of steric bulk on thermal stability, volatility and reactivity. Trimethylgermyl substituents were employed rather than trimethylsilyl substituents because $\{(Me_3Ge)Li(THF)_2\}_2$ can be prepared in good yield (*vide infra*) without the use of highly toxic organomercury reagents. By contrast, trimethylsilyllithium is only accessible via $[Hg(SiMe_3)_2]$,[52] or as an adduct with strongly coordinating hexamethylphosphoramide (HMPA) or tris(*N*,*N*-tetramethylene)phosphoric triamide (TPPA).[53,54]

It is also notable that boranes bearing a combination of bulky silyl and sterically unencumbered trimethylgermyl groups may be particularly suitable as ALD precursors since bulky silyl groups can be expected to impart thermal stability, while the less-hindered B-GeMe$_3$ linkages can serve as sites for initial reactivity. Furthermore, these boranes can be expected to be more volatile than boranes bearing only bulky silyl groups due to their lower molecular weight. To the best of our knowledge, there are less than a dozen di(silyl/germyl)amidoboranes reported in literature,[50,52,55-60] and only 4 have been crystallographically characterized (Table 1).

RESULTS & DISCUSSION

Synthesis and Structures of Alkali Metal Silyl and Germyl Compounds. The alkali metal silyl and germyl compounds hypersilyl lithium, $\{(Me_3Si)_3Si\}Li(THF)_3$ (**1**), supersilyl sodium, (^{t}Bu$_3$Si)Na(THF)$_n$ (**2**; n = 2-3), and trimethylgermyllithium, $\{Me_3GeLi(THF)_2\}_2$ (**3**), were used for the synthesis of the silyl- and germyl-substituted boranes in this work (*vide infra*). Hypersilyllithium (**1**) was prepared in two steps from $SiCl_4$ and Me_3SiCl as previously reported,[61] and supersilyl sodium (**2**) was prepared via the multistep synthesis reported by Wiberg and coworkers.[62] THF-solvated trimethylgermyllithium (**3**) was prepared by deprotonation of Me_3GeH with ^{t}BuLi in THF at –20 °C, and was isolated as a pyrophoric white solid in 82% yield. This synthesis is based on an in situ synthesis described by E. Piers *et al*.[63] Solid **3** is stable under argon for several days at 20 °C, and months at –30 °C, but decomposes entirely over several hours under vacuum, presumably due to loss of THF followed by rapid decomposition (solutions of base-free Li-GeMe$_3$ in pentane, prepared from $Hg(GeMe_3)_2$ and activated lithium, are reported to require storage in the dark at –30°C).[64]

Single crystals of (^{t}Bu$_3$Si)Na(THF)$_2$ (**2**) were grown from a saturated hexanes solution stored at –30 °C (Figure 1), revealing a monomeric structure with a coordination number of three at sodium. The sum of C-Si-C angles in the ^{t}Bu$_3$Si- groups (avg. 318.4°) is larger than the sum of Si-Si-Si angles in the previously reported crystal structure of **1** (307.2(1)°),[61] consistent with the increased steric bulk of supersilyl versus hypersilyl substituents. This structure of **2** (space group $P2_1/c$) is comparable to the previously reported structure (space group *P-1*),[62] including similar close contacts (≥2.768 Å) between sodium and the hydrogen atoms of the Si^{t}Bu$_3$ group in a neighbouring molecule.

X-ray quality crystals of $\{Me_3GeLi(THF)_2\}_2$ (**3**) were obtained from hexanes at –30 °C, revealing a dimeric structure, with trimethylgermyl anions bridging between the lithium centres (Figure 2). The Li_2Ge_2 core is rhombohedral, with acute Li–Ge–Li and obtuse Ge–Li–Ge angles (59.37(9) and 120.63(9)°, respectively). The Li(1)–Ge(1) and Li(1)–Ge(1') distances in **1** are 2.731(3) and 2.745(2) Å. A related dimeric structure was reported for $\{(^t$BuMe$_2$Si)$_2$HGe)Li(THF)$\}_2$, but in this case the H substituents on germanium bridge between Ge and Li, and the Li–Ge distances are shorter (2.650(6) and 2.675(6) Å).[65] Shorter Li–Ge distances were also observed in the monomeric tris(hydrocarbyl)germyl lithium compound Ph^{t}BuMeGeLi(sparteine) (2.57(2) Å),[66] as well as in monomeric $Ph_2(Me_3Ge)GeLi(THF)_3$ (2.683(8) Å)[67] and $(Me_3Si)_3GeLi(THF)_3$ (2.666(6) Å),[68] and trimeric $[\{(Me_3Si)_3Ge\}Li]_3$ (2.61(1)-2.62(1) Å).[69] However, the Li–Ge

distances in **3** are comparable to those in $Ph_3GeLi(THF)(tmeda)$ (2.732(6) Å) and $Ph_3GeLi(OEt_2)_3$ (2.758(8) Å).[56,70] The elongated Ge–Li distances in **3** are presumably due to the dimeric structure, combined with a coordination number of four at lithium (the coordination number of lithium is 2 or 3 in the aforementioned dimeric or trimeric germyl compounds). The sum of the C–Ge–C angles for each of the germyl groups in **4** is 295.7(2)°, which is slightly less than that in the aforementioned bulky tris(hydrocarbyl)germyl lithium compound (303.2(1)°).

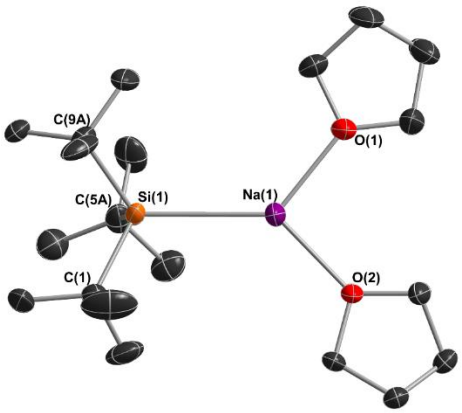

Figure 1. X-ray crystal structure of (^{t}Bu$_3$Si)Na(THF)$_2$ (**2**) with ellipsoids at 50% probability. Space group $P2_1/c$. R_1 = 0.0541. Only one of three independent molecules in the unit cell is shown. Each of the molecules displayed disorder at the carbon atoms of the THF rings and/or the methyl carbons of the *tert*-butyl groups; in each case, only the major disorder component (>50%) is shown. All hydrogen atoms have been omitted for clarity. Select bond distances (Å) and angles (°): Na(1)-Si(1) 2.912(1); Na(1)-O(1) 2.294(2); Na(1)-O(2) 2.286(2); C(1)-Si(1)-C(5A) 100.8(1); C(5A)-Si(1)-C(9A) 105.0(2); C(9A)-Si(1)-C(1) 109.5(1).

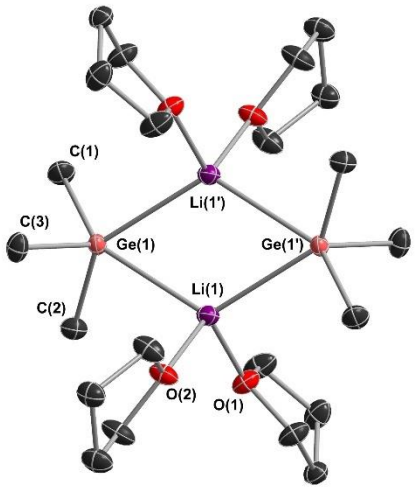

Figure 2. X-ray crystal structure of {Me$_3$GeLi(THF)$_2$}$_2$ (**3**) with ellipsoids at 50% probability. Space group *P*-1. All hydrogen atoms have been omitted for clarity. R_1 = 0.0237. Select distances (Å) and angles (°): Ge(1)-Li(1) 2.731(3); Ge(1)-Li(1') 2.745(2); Ge(1)···Ge(1') 4.7579(8); Li(1)···Li(1') 2.712(4); Li(1)-O(1) 1.942(3); Li(1)-O(2) 1.937(3); Li(1)-Ge(1)-Li(1') 59.37(9); Ge(1)-Li(1)-Ge(1') 120.63(9); O(1)-Li(1)-O(2) 102.8(1); C(1)-Ge(1)-C(2) 96.72(7); C(1)-Ge(1)-C(3) 99.82(7); C(2)-Ge(1)-C(3) 99.18(7).

Synthesis and Structures of Silyl and Germyl Boranes. The reaction of dichloro(dimethylamido)borane with two equivalents of **1** afforded previously reported {(Me$_3$Si)$_3$Si}$_2$B(NMe$_2$) (**4**; Scheme 2),[57] which was crystallized from a concentrated hexanes solution at –30 °C in 90% yield. In the solid state, compound **4** (Figure 3; the solid-state structure of **4** has not previously been reported) features a 3-coordinate boron center bound to the dimethylamido group and two hypersilyl groups in a trigonal planar geometry, with the sum of angles totaling 360.0°. The most obtuse angle about the boron center is that between the two bulky hypersilyl groups (129.9(4)°). The B-Si bond distances in **4** (2.075(8) and 2.099(7) Å) are within the range reported for other silylboranes (1.851(3)-2.131(2) Å),[71] and the B–N bond distance (1.423(9) Å) is comparable to those in other (dimethylamido)borane compounds (1.360(2)-1.451(4) Å),[72] indicative of appreciable double bond character between B and N, despite rotation of the CNC plane by 18.7° relative to the SiBSi plane to accommodate the steric bulk of the hypersilyl groups. However, it is notable that the NMe$_2$ group in **4** is rotated out of the EBE (E = Si or Ge) plane to a lesser degree than in the other structurally characterized (R$_3$E)$_2$B(NR'$_2$) compounds, (Ph$_3$Ge)$_2$B(TMP) (TMP = tetramethylpiperidinyl),[56] {(Me$_3$Si)$_2$Si(SiMe$_2$)$_2$Si(SiMe$_3$)$_2$}B(TMP)[59] and {Ph$_2$Si(SiMe$_2$)$_n$SiPh$_2$}B(TMP) (n = 2 or 3),[60] all of which bear a sterically bulky TMP group (see Table 1).

Scheme 2. Synthesis of the silyl- and germyl-substituted amidoboranes, {(Me$_3$Si)$_3$Si}$_2$B(NMe$_2$) (**4**), (^{t}Bu$_3$Si)B(NMe$_2$)Cl (**5**), (^{t}Bu$_3$Si)B(NMe$_2$)F (**6**), and (^{t}Bu$_3$Si)(Me$_3$Ge)B(NMe$_2$) (**7**).

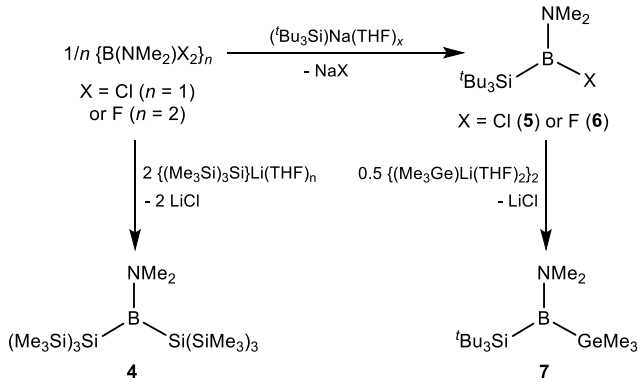

In an attempt to synthesize bis(supersilyl)(dimethylamido)borane (the supersilyl analogue of **4**), B(NMe$_2$)Cl$_2$ was reacted with 2 equivalents of (^{t}Bu$_3$Si)Na(THF)$_n$. However, this reaction only installed one supersilyl group on boron, even after 48 hours at 80 °C, forming (^{t}Bu$_3$Si)B(NMe$_2$)Cl (**5**) as a clear and colourless oil. This outcome can be attributed to the greater steric bulk of supersilyl versus hypersilyl substituents, and **5** was isolated in 72% yield from the reaction of B(NMe$_2$)Cl$_2$ with ≥1.25 equivalents of (^{t}Bu$_3$Si)Na(THF)$_n$ (mild heating was required to consume less-reactive {B(NMe$_2$)Cl$_2$}$_2$ present in the solution of B(NMe$_2$)Cl$_2$). Compound **5** afforded an ^{11}B{^{1}H} NMR signal at 41.61 ppm, which is similar to that of other reported silylamidohaloboranes (40.7-48.4 ppm).[52,55,59,73,74]

The reaction of $\{B(NMe_2)F_2\}_2$ with 2 equivalents of $(^tBu_3Si)Na(THF)_n$ was also attempted to explore whether the target bis(supersilyl)(dimethylamido)borane might be accessible due to the greater lattice enthalpy of sodium fluoride versus sodium chloride.[75] However, this reaction only afforded $(^tBu_3Si)B(NMe_2)F$ (**6**), which was isolated in 93% yield via the reaction of $\{B(NMe_2)F_2\}_2$ with 1.5 equivalents of the supersilylsodium reagent at room temperature.

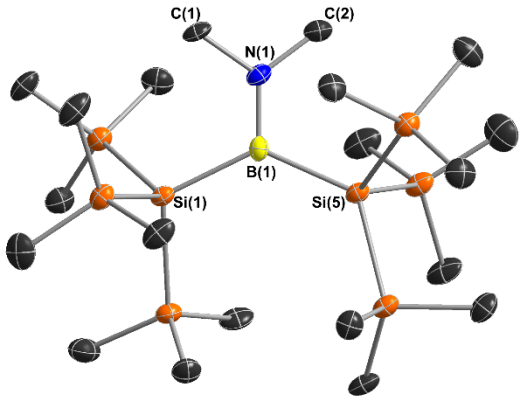

Figure 3. X-ray crystal structure of $\{(Me_3Si)_3Si\}_2B(NMe_2)$ (**4**) with ellipsoids at 50% probability. Space group *Pn*. R_1 = 0.0626. All hydrogen atoms have been omitted for clarity. Select bond lengths (Å) and angles (°): B(1)-N(1) 1.423(9); B(1)-Si(1) 2.075(8); B(1)-Si(5) 2.099(7); N(1)-C(1) 1.475(8); N(1)-C(2) 1.475(8); Si(1)-B(1)-Si(5) 129.9(4); Si(5)-B(1)-N(1) 114.3(5); N(1)-B(1)-Si(1) 115.7(5); C(1)-N(1)-C(2) 109.6(5).

The mixed silyl- and germyl-substituted amidoborane, $(^tBu_3Si)(Me_3Ge)B(NMe_2)$ (**7**), was prepared from the 2:1 reaction between $(^tBu_3Si)B(NMe_2)Cl$ (**5**) and $\{Me_3GeLi(THF)_2\}_2$ (**2**) at room temperature. To isolate pure **7** from this reaction, it was found to be critical that $B(NMe_2)Cl_2$ be completely consumed during the preparation of **5**, as trace amounts of remaining $\{B(NMe_2)Cl_2\}_2$ resulted in the formation of a product with an $^{11}B\{^1H\}$ NMR chemical shift of –13 ppm, which was identified as $\{(Me_3Ge)_3B(NMe_2)\}Li(THF)_2$ (**8**, *vide infra*).

During isolation of **7**, single crystals formed within the oil (the crude reaction product) remaining after centrifugation of the reaction mixture and removal of volatiles. The X-ray crystal structure of **7** features two independent molecules in the unit cell, each with a 3-coordinate boron center bound to the dimethylamido, supersilyl, and trimethylgermyl groups in a trigonal planar geometry (Figure 4). The B-N bond distances (1.39(1) Å in both independent molecules) fall within the range for other $(R_3E)_2B(NR'_2)$ compounds (Table 1), and the CNC/EBE interplanar angles (6.5 and 12.6°) are the smallest in Table 1.

Given the successful synthesis of $\{(Me_3Si)_3Si\}_2B(NMe_2)$ (**4**) and $(^tBu_3Si)(Me_3Ge)B(NMe_2)$ (**7**), we were interested to determine whether less sterically encumbered $(Me_3Ge)_2B(NMe_2)$ might be accessible. Therefore, the NMR-scale reaction between $B(NMe_2)Cl_2$ and 1 equivalent of $\{Me_3GeLi(THF)_2\}_2$ (**3**) was carried out, resulting in the rapid formation of a white precipitate and a mixture of species in the $^{11}B\{^1H\}$ NMR spectrum, including two major peaks: a broad peak at 45 ppm and a sharp peak at –12 ppm. The same two products were formed via slow addition of a solution of $\{Me_3GeLi(THF)_2\}_2$ (1 equiv.) to $B(NMe_2)Cl_2$ at –78 °C, and all attempts to isolate the compound that gave rise to the peak at 45 ppm were unsuccessful.

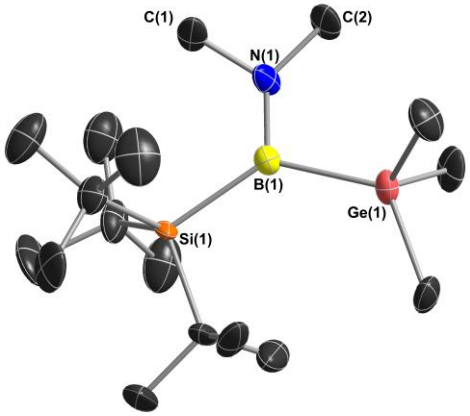

Figure 4. X-ray crystal structure of $(^tBu_3Si)(Me_3Ge)B(NMe_2)$ (**7**) with ellipsoids at 50% probability. Space group $Pna2_1$. R_1 = 0.0970. Only one of two independent molecules in the unit cell is shown. All hydrogen atoms are omitted for clarity. Select bond lengths (Å) and angles (°): B(1)-N(1) 1.39(1); B(1)-Si(1) 2.12(3); B(1)-Ge(1) 2.15(3); N(1)-C(1) 1.40(3); N(1)-C(2) 1.44(3); Si(1)-B(1)-Ge(1) 129.8(8); Ge(1)-B(1)-N(1) 109.5(17); N(1)-B(1)-Si(1) 120.6(18); C(1)-N(1)-C(2) 105.2(16).

The reaction between $B(NMe_2)Cl_2$ and **3** was repeated on a larger scale using a 1:1.5 ratio of the reactants (Scheme 3), and after removal of volatiles *in vacuo*, dissolution in pentane and filtration, colourless needle crystals suitable for X-ray diffraction studies grew from the supernatant at –30 °C. This product, with a ^{11}B NMR chemical shift of –13 ppm, was determined to be the lithium borate $\{(Me_3Ge)_3B(NMe_2)\}Li(THF)_2$ (**8**; Figure 5), in which the solvated lithium cation forms a contact ion pair with the amido group on boron. However, the quality of the crystallographic data is insufficient for more detailed discussion. Related reactivity has been reported by Nöth and coworkers, who found that reactions of $BMe_{3-n}(OMe)_n$ (n = 1-3) with trimethylsilyl lithium in varying stoichiometries afforded lithium silylborate salts, $Li[BMe_{3-n}(SiMe_3)_{n+1}]$ (n = 1-3), rather than $BMe_{3-n}(SiMe_3)_n$ boranes.[76,77]

Scheme 3. Synthesis of the tri(germyl)(amido)borate $\{(Me_3Ge)_3B(NMe_2)\}Li(THF)_2$ (**8**) and the di(germyl)(amido)borane $(Me_3Ge)_2B(TMP)$ (**9**).

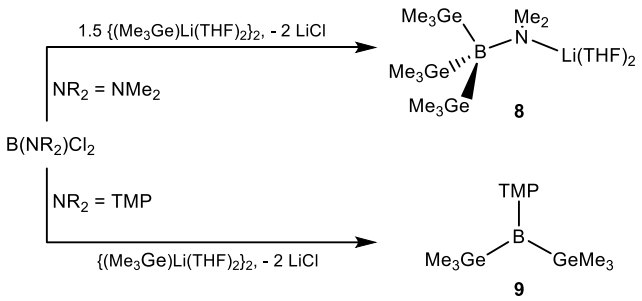

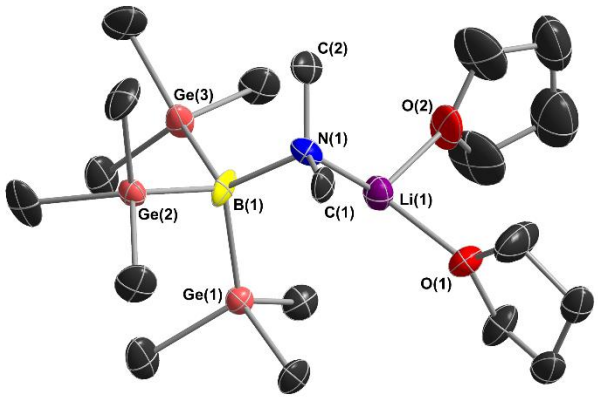

Figure 5. X-ray crystal structure of $\{(Me_3Ge)_3B(NMe_2)\}Li(THF)_2$ (**8**) with ellipsoids at 50% probability. Space group *P*1. R1 = 0.0668. Only one of six independent molecules in the unit cell is shown. Two of the molecules displayed disorder at the carbon atoms of the trimethylgermyl groups. All hydrogen atoms have been omitted for clarity. Select bond distances (Å) and angles (°): Ge(1)-B(1) 2.07(2); Ge(2)-B(1) 2.10(2); Ge(3)-B(1) 2.12(2); B(1)-N(1) 1.68(2); N(1)-C(1) 1.42(2); N(1)-C(2) 1.44(2); N(1)-Li(1) 1.96(3); Li(1)-O(1) 2.00(4); Li(1)-O(2) 2.02(3); Ge(1)-B(1)-Ge(2) 106.9(8); Ge(2)-B(1)-Ge(3) 105.3(7); Ge(3)-B(1)-Ge(1) 107.1(10); B(1)-N(1)-Li(1) 97.3(13); C(1)-N(1)-C(2) 112.1(15); N(1)-Li(1)-O(1) 118.2(18); N(1)-Li(1)-O(2) 124.6(18).

In contrast to the aforementioned reactions with $B(NMe_2)Cl_2$, reaction of bulkier $B(TMP)Cl_2$ (TMP = 2,2,6,6-tetramethylpiperidinyl) with 1 equivalent of $\{Me_3GeLi(THF)_2\}_2$ (**3**) afforded the target di(germyl)(amido)borane, $(Me_3Ge)_2B(TMP)$ (**9**; Scheme 3). Compound **9** gives rise to broad singlet in the $^{11}B\{^1H\}$ NMR spectrum at 63.52 ppm, and X-ray quality crystals were obtained from a concentrated pentane solution at –30 °C. The structure of **9** (Figure 6) contains two independent molecules in the unit cell, each with the sum of the angles about boron totaling 360.0°. The B-N distances in compound **9** (1.397(4) and 1.396(4) Å in the two independent molecules) are equivalent within error to that in previously reported $(Ph_3Ge)_2B(TMP)$, (1.409(3) Å). However, the CNC/GeBGe interplanar angles in **9** (18.3 and 20.4°) are significantly less than that in the more sterically hindered triphenylgermyl analogue (34.5°).

Borane Volatility and Thermal Stability. The volatility and thermal stability of $\{(Me_3Si)_3Si\}_2B(NMe_2)$ (**4**) was assessed to determine its potential viability as an ALD precursor. Pure **4** sublimed cleanly at 85 °C at a pressure of 10 mTorr. The thermal stability of **4** was evaluated by heating a pure solid sample in a J. Young NMR tube under static argon for 24 hours, followed by ^1H NMR spectroscopy in C_6D_6. These tests revealed that **4** is stable for 24 hours at 155 °C (higher temperatures were not investigated). Thermogravimetric analysis (TGA) of **4** was also carried out between 40 and 400 °C (Figure 7), revealing a $T_{50\%}$ temperature (the temperature at which 50% of the sample mass has been lost) of 274 °C. The single mass loss step in the TGA and the low residual mass above 300 °C (1-2%) is consistent with clean volatilization and thermal stability on the timescale of the TGA experiment.

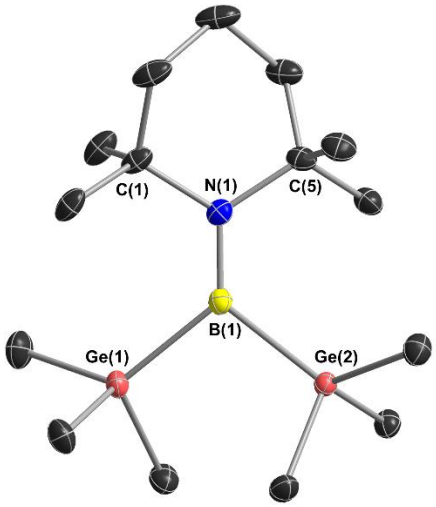

Figure 6. X-ray crystal structure of $(Me_3Ge)_2B(TMP)$ (**9**) with ellipsoids at 50% probability. Space group $P2_1/c$. $R_1 = 0.0355$. Only one of two independent molecules in the unit cell is shown. All hydrogen atoms have been omitted for clarity. Select bond lengths (Å) and angles (°): B(1)-N(1) 1.397(4); B(1)-Ge(1) 2.122(3); B(1)-Ge(2) 2.131(3); N(1)-C(1) 1.523(4); N(1)-C(2) 1.527(4); Ge(1)-B(1)-Ge(2) 104.9(1); Ge(2)-B(1)-N(1) 127.2(2); N(1)-B(1)-Ge(1) 127.9(2); C(1)-N(1)-C(2) 114.7(2).

Table 1. ^{11}B NMR chemical shifts, B-N bond distances, and CNC/EBE interplanar angles for crystallographically characterized $(R_3E)_2B(NR'_2)$ boranes, where E is Si or Ge.

Compound	^{11}B NMR Chemical Shift (ppm)	B-N Distance (Å)	Interplanar Angle (°)
$(Ph_3Ge)_2B(TMP)$[56]	64.0 (C_6D_6)	1.409(3)	34.5
$\{(Me_3Si)_2Si\text{-}(SiMe_2)_2\text{-}(Me_3Si)_2Si\}B(TMP)$[59]	72.1 (C_6D_6)	1.406(7)	40.4
$\{Ph_2Si\text{-}(SiMe_2)_2\text{-}Ph_2Si\}B(TMP)$[60]	63.77 (CD_2Cl_2)	1.408(2)	31.6
$\{Ph_2Si\text{-}(SiMe_2)_3\text{-}Ph_2Si\}B(TMP)$[60]	66.30 (CD_2Cl_2)	1.409(3)	36.1
$\{(Me_3Si)_3Si\}_2B(NMe_2)$ (**4**)	60.65 (C_6D_6)	1.423(9)	18.7
$(^tBu_3Si)(Me_3Ge)B(NMe_2)$ (**7**)	59.88 (C_6D_6)	1.39(1), 1.39(1)	6.5, 12.6
$(Me_3Ge)_2B(TMP)$ (**9**)	63.52 (C_6D_6)	1.397(4), 1.396(4)	18.3, 20.4

In comparison to compound **4**, $(^tBu_3Si)(Me_3Ge)B(NMe_2)$ (**7**) is more volatile, and distilled at 45 °C at a pressure of 10 mTorr. Compound **7** also has the advantage[24,78,79] of a melting point near room temperature (~40 °C). Thermal stability tests (conducted as described above for compound **4**) demonstrated that **7** is stable for 24-hour periods at 95 °C in the absence of light. However, **7** was significantly decomposed (~50%; presumably

due to autocatalytic decomposition) after 5 days at 95 °C, demonstrating diminished thermal stability relative to **4**. A neat sample of **7** heated at 95 °C for 6 days under partial pressure was found to form (^{t}Bu$_3$Si)B(NMe$_2$)(CH$_3$) as the major soluble product (Figures S36-43; the same compound was formed via the reaction of **5** with 1 equiv. of MeLi), accompanied by an unidentified white precipitate.¶ TGA of **7** (Figure 7) revealed a $T_{50\%}$ temperature of 194 °C but the rate of mass loss decreased significantly above 200 °C, and the TGA profile is suggestive of a combination of volatilization and thermal decomposition. However, it is notable that only 1.5% of the original mass remained at 400 °C, indicating that the decomposition products volatilize at elevated temperature.

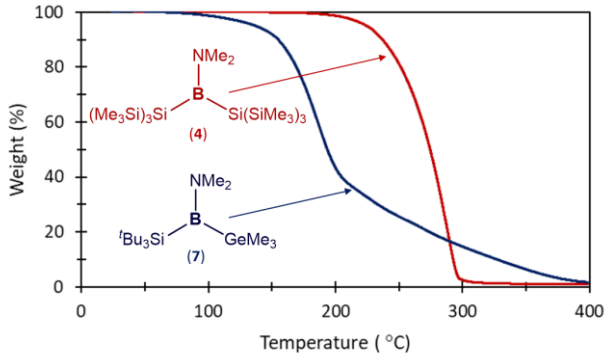

Figure 7. TGA of {(Me$_3$Si)$_3$Si}$_2$B(NMe$_2$) (**4**) and (^{t}Bu$_3$Si)(Me$_3$Ge)B(NMe$_2$) (**7**). Ramp rate = 10 °C/min; starting weights = 3.481 mg (**4**), 3.306 mg (**7**).

In contrast to **4** and **7**, compound **9** partially decomposed during attempted sublimation at 70 °C and 10 mTorr, and completely decomposed after heating in the dark at 110 °C for 24 hours. TGA was not obtained due to the poor thermal stability of **9**. Decreasing thermal stability in the order **4** > **7** > **9** highlights the ability of bulky silyl groups to enhance the thermal stability of di(silyl/germyl)(amido)boranes.

Reactivity of Germyl- and Silyl-substituted Boranes. Solution reactions between **4** and excess BCl$_3$ (in heptane) or BBr$_3$ were conducted and monitored by ^{1}H and ^{11}B{^{1}H} NMR spectroscopy (and in some cases ^{13}C{^{1}H} and ^{29}Si-^{1}H HMBC NMR spectroscopy), and the results are summarized in Table S3 in the supporting information. The reaction of **4** with BCl$_3$ resulted in slow consumption of **4** at room temperature to form a mixture of soluble products, including B(NMe$_2$)Cl$_2$, {B(NMe$_2$)Cl$_2$}$_2$, and {(Me$_3$Si)$_3$Si}BCl$_2$ (confirmed based on their ^{1}H and ^{11}B NMR peak positions, which are 2.38 and 30.9 ppm, 2.19 and 10.4 ppm, and 0.26 and 79.2 ppm, respectively). However, (Me$_3$Si)$_3$SiCl (^{13}C NMR δ –0.52 ppm, ^{29}Si NMR δ –12.51 and –11.5 ppm) was not observed. The reaction of **4** with BBr$_3$ proceeded analogously, but the only identified product was B(NMe$_2$)Br$_2$ (^{1}H and ^{11}B NMR chemical shifts of 2.34 and 25.6 ppm, respectively), and (Me$_3$Si)$_3$SiBr (^{1}H NMR δ 0.29 ppm) was not observed.† Both reactions also afforded an unidentified byproduct with an ^{11}B NMR chemical shift of 62.23 or 62.92 ppm, respectively. The substantial number of minor products from these reactions, especially the latter reaction, may indicate some degree of Si-Si bond cleavage within the hypersilyl ligand.

Solution reactions of **7** with excess BCl$_3$ or BBr$_3$ were also investigated. Compound **7** reacted rapidly (within 10 minutes) with both boron trihalides, and multiple products (~5) were formed in each of these reactions. In the reaction with BCl$_3$, identified products were B(NMe$_2$)Cl$_2$, {B(NMe$_2$)Cl$_2$}$_2$, (^{t}Bu$_3$Si)BCl$_2$, and ^{t}Bu$_3$SiCl, whereas Me$_3$GeCl was not observed (^{13}C{^{1}H} NMR δ 4.56 ppm). In the reaction of **7** with BBr$_3$, the products B(NMe$_2$)Br$_2$, (^{t}Bu$_3$Si)BBr$_2$, and ^{t}Bu$_3$SiBr were identified, while Me$_3$GeBr (^{1}H NMR δ 0.51 ppm) was not present.† Similar to reactions with **4**, both reactions with **7** afforded an unidentified room-temperature-volatile byproduct with an ^{11}B NMR chemical shift of 62.24 or 62.92 ppm, respectively. The reaction of **7** with BBr$_3$ also afforded an off-white precipitate which was soluble in THF. However, attempts to identify or crystallize this product were unsuccessful.‡

The formation of {B(NMe$_2$)X$_2$}$_n$ (X = Cl or Br) in these reactions implies that step 1 in Scheme 1 proceeds as intended. However, the observation of {(Me$_3$Si)$_3$Si}BCl$_2$ and (^{t}Bu$_3$Si)BX$_2$ (X = Cl or Br) suggests that the (R$_3$E)$_2$BX product from step 1 undergoes substituent redistribution with BX$_3$ to afford (R$_3$E)BX$_2$, in preference to R$_3$EX elimination. Nevertheless, the formation of ^{t}Bu$_3$SiX in reactions of **7** with BX$_3$ (X = Cl or Br) indicates that R$_3$SiX reductive elimination can take place, possibly from (^{t}Bu$_3$Si)BX$_2$ as previously described.[46]

Although the solution reactions of **4** or **7** with boron trihalides did not afford elemental boron, ALD reactions are typically carried out at higher temperature than solution reactions, which may promote the R$_3$EX (E = Si or Ge; X = Cl or Br) elimination required in step 2 of Scheme 1. Furthermore, in each cycle of an ALD process, the surface is sequentially supplied with an excess of the precursor (e.g. **4** or **7**) and then the co-reactant (BX$_3$ in this work), which can lead to a different reaction outcome compared to solution reactivity, where the ratio of the reactants does not typically oscillate over the course of the reaction. It is also notable that deviations between solution and ALD reactivity can arise from the requirement for adsorption of the precursor and/or co-reactant on the substrate surface during film growth in ALD, and differences in the structure and reactivity of surface species formed during ALD relative to intact molecules in solution reactions. Furthermore, in ALD, reaction byproducts must be volatile in order to generate a film of reasonable purity whereas in solution deposition reactions they must be soluble, and in solution reactions, unlike ALD reactions, precipitation of an oligomeric/polymeric inorganic product can occur prior to complete reaction (e.g. before complete removal of the ligands present in the precursor), hindering further reactivity.

Consequently, ALD reactor studies using more thermally robust **4** in combination with BCl$_3$ or BBr$_3$ were carried out using both 100 nm SiO$_2$ on Si (SiO$_2$/Si) and hydrogen-terminated silicon (H-Si) substrates. These experiments utilized a reactor pressure of approximately 240 mTorr (achieved using a total argon flow of 80 sccm), substrate temperatures of 150 and 300 °C, and 1000 ALD cycles. Compound **4** was delivered at 135 °C using 4 second pulses, BBr$_3$ was delivered at room temperature using 0.05s pulses, and BCl$_3$ gas was delivered using 5 second pulses at a flow rate of 5 sccm. However, minimal deposition (≤2 nm) was observed at both temperatures.§

Summary and Conclusions. Boranes featuring bulky hypersilyl {$(Me_3Si)_3Si$} or supersilyl ($^tBu_3Si$) groups, and/or sterically unencumbered trimethylgermyl substituents, were synthesized for investigation as potential boron ALD precursors. Trimethylgermyl groups were used in this work, rather than trimethylsilyl groups, due to the straightforward synthesis of $\{Me_3GeLi(THF)_2\}_2$ (**3**) from trimethylgermane and *tert*-butyllithium. By contrast, $LiSiMe_3$, which was not used in this work, is synthesized via highly toxic and volatile $Hg(SiMe_3)_2$.[52] Other starting materials in this work, hypersilyl lithium, $\{(Me_3Si)_3Si\}Li(THF)_3$ (**1**),[61] and supersilyl sodium, ($^tBu_3Si$)$Na(THF)_n$ (**2**; n = 2-3),[62] were prepared as previously reported, and both **2** (n = 2; space group $P2_1/c$) and **3** were crystallographically characterized.

The previously reported di(silyl)(amido)borane $\{(Me_3Si)_3Si\}_2B(NMe_2)$ (**4**)[57] was synthesized via the reaction of $B(NMe_2)Cl_2$ with 2 equiv. of $\{(Me_3Si)_3Si\}Li(THF)_3$ (**1**). By contrast, reactions of $B(NMe_2)Cl_2$ with 2 equiv. of ($^tBu_3Si$)$Na(THF)_n$ (**2**; n = 2-3) only afforded ($^tBu_3Si$)$B(NMe_2)Cl$ (**5**) with a single silyl substituent, and reactions with $\{B(NMe_2)F_2\}_2$ proceeded analogously to form ($^tBu_3Si$)$B(NMe_2)F$ (**6**). Subsequent reactions of **5** with 0.5 equivalents of $\{Me_3GeLi(THF)_2\}_2$ (**3**) afforded ($^tBu_3Si$)(Me_3Ge)$B(NMe_2)$ (**7**); the first example of a mixed silyl/germyl borane. Attempts to synthesize $(Me_3Ge)_2B(NMe_2)$ from the 1:1 reaction of $B(NMe_2)Cl_2$ with $\{Me_3GeLi(THF)_2\}_2$ afforded a mixture of two major products, one of which was identified as the tri(germyl)(amido)borate $\{(Me_3Ge)_3B(NMe_2)\}Li(THF)_2$ (**8**); this compound was generated cleanly from the 1:1.5 reaction of $B(NMe_2)Cl_2$ with $\{Me_3GeLi(THF)_2\}_2$. By contrast, reaction of more sterically encumbered $B(TMP)Cl_2$ with one equivalent of $\{Me_3GeLi(THF)_2\}_2$ afforded the di(germyl)(amido)borane, $(Me_3Ge)_2B(TMP)$ (**9**). Boranes **4**, **7** and **9**, and borate **8**, were crystallographically characterized.

Borane **4** sublimed cleanly at 85 °C (10 mTorr), and was stable for 24 hours at 155 °C. It also underwent clean volatilization by TGA, with a $T_{50\%}$ temperature (the temperature at which 50% of the sample mass has been lost) of 274 °C. By contrast, compound **7**, which has a lower molecular mass and lower symmetry (approx. C_s vs C_{2v}), has a melting point of just 40 °C, and distilled cleanly at 45 °C (10 mTorr). However, compound **7** is also less sterically stabilized than **4**, and was 50% decomposed after 5 days at 95 °C in the dark. Additionally, the TGA profile of **7** is indicative of a combination of volatilization and thermal decomposition. The least sterically hindered borane, compound **9**, partially decomposed during attempted sublimation at 70 °C (10 mTorr) and was completely decomposed after heating in the dark at 110 °C for 24 hours. Decreasing thermal stability in the order **4** > **7** > **9** highlights the ability of bulky silyl groups to enhance the thermal stability of the di(silyl/germyl)(amido)boranes. Compound **4** is sufficiently volatile and thermally stable to be used as an ALD precursor, whereas, the thermal stability of **7** is insufficient for practical use as an ALD precursor.

In solution, **4** and **7** reacted with excess BCl_3 or BBr_3 at room temperature, and the most rapid reaction was between **7** and BBr_3. The observed reaction byproducts (not all of which were identified) suggest that exchange of both the amido and the silyl (and presumably also germyl) groups in **4** and **7** with bromo or chloro substituents in the BX_3 reagent can take place, and that $^tBu_3SiX$ (X = Cl or Br) reductive elimination also occurs, possibly from ($^tBu_3Si$)BX_2 as previously described.[46] However, these reactions did not form elemental boron, and attempted ALD using **4** in combination with BCl_3 and BBr_3 at 150 and 300 °C did not result in significant film growth. Future work will investigate the potential of di(silyl/germyl)(amido)boranes for metal boride ALD in combination with metal halide precursors, and the synthesis of more thermally stable (supersilyl)(silyl/germyl)(amido)boranes.

EXPERIMENTAL SECTION

All synthesis was carried out using standard techniques under an argon atmosphere in an MBraun Unilab glovebox equipped with a –30 °C freezer, or on a double manifold vacuum line equipped with an Edwards RV12 vacuum pump. The vacuum was measured periodically using a Kurt J. Lesker 275i convection enhanced Pirani gauge and was always below 10 mTorr. Residual oxygen and moisture was removed from the argon stream to the vacuum line by passage through an Oxisorb-W scrubber from Matheson Gas Products. All compounds synthesized in this work are air- and moisture-sensitive (in some cases pyrophoric) and should therefore be handled and stored under an inert atmosphere. All compounds are stable for prolonged periods when stored at –30 °C, and compounds **4** and **7** were shown to be stable at room temperature over periods of a year or three months, respectively.

Preparations of THF-coordinated hypersilyllithium (**1**)[61,80], THF-coordinated supersilylsodium (**2**)[62,81], and $B(TMP)Cl_2$[82] were conducted according to literature procedures. Bis(hypersilyl)(dimethylamido)borane, $\{(Me_3Si)_3Si\}_2B(NMe_2)$ (**4**), was prepared following literature procedures,[31,57] and was fully characterized (multinuclear NMR spectroscopy, X-ray crystallography and combustion elemental analysis; see below; previous characterization was limited to ^{11}B NMR spectroscopy and combustion elemental analysis).[57] The preparations of dichloro(dimethylamido)borane and (dimethylamido)difluoroborane were slightly modified from the literature procedures[83] to avoid the handling of gaseous BX_3, and their detailed synthesis and characterization are described below. All commercial reagents (Li, Na, Me_3SiCl, $SiCl_4$, MeLi (1.6M in Et_2O), $^tBu_2SiHCl$, KF, KHF_2, ^tBuLi (1.7M in pentane), ^nBuLi (1.6M in hexanes), Br_2, $LiAlH_4$, Me_3GeBr, BCl_3 (1.0M in heptane), $BF_3{\cdot}OEt_2$, BBr_3, BI_3, $B(NMe_2)_3$, TMPH) were purchased from Sigma Aldrich and stored under argon. TMPH was dried under sieves and distilled before use, whereas all other reagents were used without further purification. Argon gas was purchased from Air Liquide.

Benzene, pentane, hexanes, toluene and tetrahydrofuran (THF) were purchased from Sigma Aldrich. These solvents were initially dried and distilled at atmospheric pressure from sodium (toluene) or sodium/benzophenone (the other four solvents). All solvents were stored over an appropriate drying agent (benzene, toluene, THF = Na/Ph_2CO; hexanes, pentane = Na/Ph_2CO/tetraglyme) and introduced to reactions or solvent storage flasks via vacuum transfer with condensation at –78 °C. C_6D_6 (99.5%) was purchased from Sigma Aldrich and was dried over sodium/benzophenone, distilled prior to use, and stored under argon.

The ALD reactor design, ALD experiment setup, substrate preparation, and methods of thin films characterization are identical to what has been previously reported,[41] except that carrier argon flows were set to 20 sccm for all delivery lines (resulting in an internal pressure of ~240 mTorr), and the 4Å molecular sieves trap was replaced by a 6" body liquid nitrogen trap (MDC Precision) to collect excess BX_3 coreactant. In all ALD experiments, the oven containing the reactor chamber was held at 150 °C. Compound **4** was delivered at 135 °C. Attempts to deliver **7** at 85 °C led to insufficient delivery, so the bubbler temperature was raised to 95 °C, leading to complete decomposition after several days. The cylinder of BCl_3 used in ALD reactor experiments was purchased from Air Liquide.

Solution NMR spectroscopy (nuclei: ^1H, ^{13}C, ^{11}B, ^{29}Si, ^{19}F) was performed on a Bruker AV-600 NMR spectrometer (for room temperature measurements) or a Bruker AV-500 NMR spectrometer (for low temperature studies). All ^1H and $^{13}C\{^1H\}$ NMR spectra were referenced to $SiMe_4$ through the resonance of the proto impurity in C_6D_6 (for ^1H NMR; 7.16 ppm) or the resonance of C_6D_6 (for ^{13}C NMR; 128.06 ppm).

$^{11}B\{^1H\}$, ^{29}Si, and ^{19}F NMR spectra were indirectly referenced by conversion of the spectral frequency of the ^1H NMR spectrum using the frequency ratio (Ξ) of each nuclei to ^1H, as described by Harris *et al*.[84] All reported ^{29}Si NMR chemical shifts were located from crosspeaks in 2D ^{29}Si-^1H HMBC NMR spectra.

Combustion elemental analyses were performed at the University of Calgary using a Perkin Elmer Model 2400 series II analyzer. Single crystal X-ray diffraction studies were conducted on crystals coated in Paratone oil and mounted on either (a) a SMART APEX II diffractometer with a 3 kW sealed-tube Mo generator and SMART6000 CCD detector (**4**), (b) a STOE IPDS II diffractometer with an image plate detector (**2**, **3**, **7**, **8**), or (c) a Bruker Dual Source D8 Venture diffractometer (**9**) in the McMaster Analytical X-ray diffraction (MAX) facility. Raw data was processed using XPREP (as part of the APEX v2.2.0 software) and solved by an intrinsic method (SHELXT).[85,86] In all cases, non-hydrogen atoms were refined anisotropically and hydrogen atoms were generated in ideal positions and then updated with each refinement cycle. All structure solutions and refinements were performed using Olex2.[87] Deposition Numbers 2372743 (for **2**), 2372744 (for **3**), 2372745 (for **4**), 2372746 (for **7**), 2372747 (for **8**), and 2372748 (for **9**) contain the supplementary crystallographic data for this paper.

{Me$_3$GeLi(THF)$_2$}$_2$ (3). The synthesis of **3** is based on an in situ synthesis described by E. Piers *et al*.[63] The synthesis generates Me_3GeH in situ from Me_3GeBr (which is easier to handle than highly volatile Me_3GeH), although comparable yields were obtained directly from Me_3GeH. **In situ synthesis of Me$_3$GeH:** A suspension of $LiAlH_4$ (580 mg, 15.3 mmol) in THF (25 ml) was prepared cautiously (addition of THF to solid $LiAlH_4$ is highly exothermic and slow addition is essential). To this was added a THF solution (15 mL) of Me_3GeBr (2.97 g, 15.1 mmol) dropwise via syringe at 0 °C. After stirring for 10 minutes at 0 °C, the mixture was cooled to –78 °C and degassed for 1 minute before warming to room temperature under static vacuum. All volatiles were then vacuum distilled through the vacuum line into a receiving flask at –78 °C. **Deprotonation of Me$_3$GeH:** After warming the resulting Me_3GeH solution to –20 °C, a solution of tert-butyllithium (1.06 g, 16.5 mmol) in pentane (10 mL) was added dropwise to the stirring solution via syringe over 5 minutes. The yellow solution was stirred at –20 °C for 10 minutes and maintained at this temperature to remove most of the volatiles *in vacuo*. Once the mixture had the appearance of a thick slurry, the flask was warmed to room temperature and the mixture was further evacuated for 30 minutes until a solid pale-yellow residue was left. The flask and adapter were then secured with electrical tape (as a precaution in case some residual solvent is present, potentially causing the pressure within the flask to exceed the pressure in the glovebox port during evacuation) and brought into a glove box. To the residue was added ca. 15 mL of hexanes. The suspension was transferred into a 20 mL vial and stored at –30 °C overnight. After decanting the solvent, the white solid was washed with 3×5 mL of cold hexanes. The resulting solid was dried under argon at room temperature in the glove box, affording **3** as a pyrophoric white solid (3.3 g, 82%). X-ray quality single crystals were grown as colourless needles from a hexanes solution at –30 °C. *Note: although compound **3** is stable indefinitely at –30 °C under argon, it decomposes under vacuum (forming a viscous grey-white oil) over a few hours, presumably due to loss of THF followed by rapid decomposition*. ^1H NMR (C_6D_6, 600 MHz, 298 K): δ 3.61 (t, 8H, CH_2CH_2O), 1.36 (m, 8H, CH_2CH_2O), 0.62 (s, 9H, $Ge(CH_3)_3$) ppm. $^{13}C\{^1H\}$ NMR (C_6D_6, 151 MHz, 298 K): δ 68.66 (s, CH_2CH_2O), 25.44 (s, CH_2CH_2O), 7.42 (s, $Ge(CH_3)_3$) ppm. **$C_{22}H_{50}Ge_2Li_2O_4$ (537.78 g·mol^{-1}):** calcd. C 49.14, H 9.37, N 0.00%; found. C 49.49, H 9.03, N 0.26%.

B(NMe$_2$)Cl$_2$. A 1.0M solution of boron trichloride in *n*-heptane (21.6 mL; 21.6 mmol of BCl_3) was added dropwise via syringe to a vigorously stirred solution of tris(dimethylamido)borane (1.23 g, 8.62 mmol) in 30 mL of *n*-pentane in a 100 mL bomb. The clear and colourless solution was stirred at room temperature for one hour, at which point the reaction was cooled to 0 °C. The volume of the solution was reduced *in vacuo* to approximately one third of the original volume (this procedure removed all of the *n*-pentane and excess BCl_3). The solution was centrifuged for 10 minutes to remove any solid dimer ($\{B(NMe_2)Cl_2\}_2$) before storing the colourless solution of dichloro(dimethylamido)borane in a vial at room temperature under argon. *Note: the concentration of the 1:x B(NMe$_2$)Cl$_2$/heptane mixture was determined by integration of the ^1H NMR signal of the product ($N(CH_3)_2$) relative to heptane (CH_3) before use in reactions (typical relative integrations (ie. x) were between 5 and 10). The $\{B(NMe_2)Cl_2\}_2$ dimer slowly crystallized out of the stock solution over time, therefore the solution was typically used within 1 week, and the concentration of the solution was determined immediately before use.* ^1H NMR (C_6D_6, 500 MHz, 298 K): δ 2.34 (s, 6H, $N(CH_3)_2$), 1.28 (m, heptane), 0.90 (t, heptane) ppm. $^{13}C\{^1H\}$ NMR (C_6D_6, 151 MHz, 298 K): δ 39.36 (s, $N(CH_3)_2$), 32.37, 29.56, 23.17, and 14.36 (s, heptane) ppm. $^{11}B\{^1H\}$ NMR (C_6D_6, 161 MHz, 298 K): δ 30.48 (s) ppm.

{B(μ-NMe$_2$)Cl$_2$}$_2$. Solutions of $B(NMe_2)Cl_2$ in *n*-heptane at room temperature always contain some dimer $\{B(NMe_2)Cl_2\}_2$ which precipitates slowly as large colourless block-shaped crystals. ^1H NMR (C_6D_6, 500 MHz, 298 K): δ 2.19 (sept, 6H, $N(CH_3)_2$, $^2J_{H,H}$ = 3.3 Hz) ppm. $^{13}C\{^1H\}$ NMR (C_6D_6, 126 MHz, 298 K): δ 34.56 (s, $N(CH_3)_2$) ppm. $^{11}B\{^1H\}$ NMR (C_6D_6, 161 MHz, 298 K): δ 10.40 (s) ppm.

{B(μ-NMe$_2$)F$_2$}$_2$. The dimer of (dimethylamido)difluoroborane was prepared analogously to $B(NMe_2)Cl_2$ using $B(NMe_2)_3$ (442 mg, 3.09 mmol) and $BF_3{\cdot}OEt_2$ (0.80 mL, 6.48 mmol). Monomeric $B(NMe_2)F_2$ dimerizes and rapidly precipitates out of solution. The precipitate was dried *in vacuo* to obtain the dimer as a white crystalline solid (846 mg, 98%). ^1H NMR (C_6D_6, 600 MHz, 298 K): δ 1.98 (s, 6H, $N(CH_3)_2$) ppm. $^{13}C\{^1H\}$ NMR (C_6D_6, 151 MHz, 298 K): δ 38.31 (s, $N(CH_3)_2$) ppm. $^{11}B\{^1H\}$ NMR (C_6D_6, 161 MHz, 298 K): δ 0.98 (m) ppm. ^{19}F NMR (C_6D_6, 565 MHz, 298 K): δ –161.85 (m) ppm.

{(Me$_3$Si)$_3$Si}$_2$B(NMe$_2$) (4). Compound **4** was prepared in 97% yield following the literature procedure.[57] X-ray quality single crystals were grown from a concentrated hexanes solution at –30 °C. ^1H NMR (C_6D_6, 600 MHz, 298 K): δ 2.97 (s, 6H, $N(CH_3)_2$), 0.37 (s, 54H, $Si(CH_3)_3$) ppm. $^{13}C\{^1H\}$ NMR (C_6D_6, 151 MHz, 298 K): δ 50.61 (s, $N(CH_3)_2$), 5.13 (s, $Si(CH_3)_3$) ppm. $^{11}B\{^1H\}$ NMR (C_6D_6, 193 MHz, 298 K): δ 60.65 (s) ppm. ^{29}Si NMR (C_6D_6, 119 MHz, 298 K): δ –9.55 (s, $Si(SiMe_3)_3$), –112.81 (s, $Si(SiMe_3)_3$) ppm. **$C_{20}H_{60}BNSi_8$ (550.20 g·mol^{-1}):** calcd. C 43.66, H 10.99, N 2.55%; found. C 43.28, H 11.03, N 2.48%.

(^{t}Bu$_3$Si)B(NMe$_2$)Cl (5). A 1:7 $B(NMe_2)Cl_2$/heptane mixture (8.0236 g of the mixture, 9.7 mmol of $B(NMe_2)Cl_2$) was diluted with approximately 5 mL of hexanes. It was then added dropwise via syringe to a bright yellow-orange solution of ^{t}Bu$_3$SiNa(THF)$_2$ (**2**; 4.442 g, 12.1 mmol) in hexanes (15 mL). Upon addition, the reaction mixture began to lighten in colour, forming a cloudy light yellow solution, and then a nearly colourless solution with a white precipitate. The reaction mixture was stirred at 50 °C overnight to allow for complete consumption of $\{B(NMe_2)Cl_2\}_2$, some of which was always present in solutions of $B(NMe_2)Cl_2$. All volatiles were removed *in vacuo* and the pale-yellow residue was redissolved in 5 mL of hexanes and centrifuged to remove NaCl. After removal of solvent *in vacuo*, the crude product was purified by distillation at 90 °C/10 mTorr to obtain pure **5** as a clear and colourless oil (2.52 g, 72%). ^1H NMR (C_6D_6, 600 MHz, 298 K): δ 2.70 (s, 6H, $N(CH_3)_2$), 1.31 (s, 27H, $C(CH_3)_3$) ppm. $^{13}C\{^1H\}$ NMR (C_6D_6, 151 MHz, 298 K): δ 45.02 (s, $N(CH_3)_2$), 41.19 (s, CMe_3), 32.84 (s, $C(CH_3)_3$) ppm. $^{11}B\{^1H\}$ NMR (C_6D_6, 193 MHz, 298 K): δ 41.61 (s) ppm. ^{29}Si NMR (C_6D_6, 119 MHz, 298 K): δ 2.18 ppm. **$C_{14}H_{33}BClNSi$ (289.77 g·mol^{-1}):** calcd. C 58.03, H 11.48, N 4.83%; found. C 57.93, H 11.37, N 4.70%.

(^{t}Bu$_3$Si)B(NMe$_2$)F (6). A solution of ^{t}Bu$_3$SiNa(THF)$_2$ (**2**; 238.4 mg, 0.922 mmol) in hexanes (10 mL) was added dropwise to a stirred room temperature suspension of $\{B(NMe_2)F_2\}_2$ (114.2 mg, 0.615 mmol) in 2 mL of hexanes. This afforded a yellow-orange solution which turned into a nearly translucent, faint yellow mixture over the course of 1 hour. The reaction was stirred for 1 additional hour at room temperature before centrifugation and removal of solvent *in vacuo*. The residue was

redissolved in pentane (4 mL) and stored at –30 °C overnight to crystallize unreacted {B(NMe$_2$)F$_2$}$_2$. The solution was decanted, dried *in vacuo* and distilled at 50 °C/10 mTorr (to separate product from excess **2**) to obtain **6** as a clear and colourless oil (235.6 mg, 93%). ^{1}H NMR (C$_6$D$_6$, 600 MHz, 298 K): δ 2.56 (d, $^4J_{H,F}$ = 1.6 Hz, 3H, N(C*H*$_3$)$_2$), 2.46 (d, $^4J_{H,F}$ = 2.1 Hz, 3H, N(C*H*$_3$)$_2$), 1.26 (s, 27H, C(C*H*$_3$)$_3$) ppm. ^{13}C{^{1}H} NMR (C$_6$D$_6$, 151 MHz, 298 K): δ 39.55 (d, $^3J_{CF}$ = 4.6 Hz, N(*C*H$_3$)$_2$), 35.58 (d, $^3J_{CF}$ = 13.8 Hz, N(*C*H$_3$)$_2$), 32.15 (s, C(*C*H$_3$)$_3$), 22.70 (s, *C*Me$_3$) ppm. ^{11}B{^{1}H} NMR (C$_6$D$_6$, 193 MHz, 298 K): δ 34.35 (d, $^1J_{B,F}$ = 130 Hz). ^{19}F NMR (C$_6$D$_6$, MHz, 298 K): δ –70.95 (m) ppm. ^{29}Si NMR (C$_6$D$_6$, 119 MHz, 298 K): δ 2.28 ppm. **C$_{14}$H$_{33}$BFNSi (273.32 g·mol^{-1}):** calcd. C 61.52, H 12.17, N 5.12%; found. C 61.53, H 12.02, N 5.55%.

(*t*Bu$_3$Si)(Me$_3$Ge)B(NMe$_2$) (7). A solution of {Me$_3$GeLi(THF)$_2$}$_2$ (**3**; 285.2 mg, 0.530 mmol) in benzene (8 mL) was added dropwise via syringe to a stirred solution of (*t*Bu$_3$Si)B(NMe$_2$)Cl (**5**; 307.4 mg, 1.06 mmol) in hexanes (4 mL) at room temperature. Over the course of one hour, the clear colourless solution became a translucent, pale yellow mixture which was stirred at room temperature overnight. The mixture was centrifuged to remove LiCl and evaporated to dryness *in vacuo*. The crude, pale yellow waxy solid was distilled at 45 °C/10 mTorr to afford **7** as a clear and colourless oil that would on occasion solidify into a crystalline white solid over approximately one hour at room temperature (302.5 mg, 77%). ^{1}H NMR (C$_6$D$_6$, 600 MHz, 298 K): δ 2.96 and 2.82 (2×s, 2×3H, N(C*H*$_3$)$_2$), 1.27 (s, 27H, C(C*H*$_3$)$_3$), 0.46 (s, 9H, Ge(C*H*$_3$)$_3$) ppm. ^{13}C{^{1}H} NMR (C$_6$D$_6$, 151 MHz, 298 K): δ 53.25 and 47.84 ppm (2×s, N(*C*H$_3$)$_2$), 33.32 (s, SiC(*C*H$_3$)$_3$), 23.64 (s, Si*C*Me$_3$), 5.11 (s, Ge(*C*H$_3$)$_3$) ppm. ^{11}B{^{1}H} NMR (C$_6$D$_6$, 193 MHz, 298 K): δ 59.88 (s) ppm. ^{29}Si NMR (C$_6$D$_6$, 119 MHz, 298 K): δ 4.43 ppm. **C$_{17}$H$_{42}$BNGeSi (372.06 g·mol^{-1}):** calcd. C 54.88, H 11.38, N 2.91%; found. C 55.25, H 11.05, N 3.30%.

{(Me$_3$Ge)$_3$B(NMe$_2$)}Li(THF)$_2$ (8). A 1:9 mixture of B(NMe$_2$)Cl$_2$ and heptane (289 mg of the mixture, 0.320 mmol of B(NMe$_2$)Cl$_2$) was diluted with approximately 5 mL of hexanes. It was then added dropwise via syringe to a stirred solution of {Me$_3$GeLi(THF)$_2$}$_2$ (**3**; 258 mg, 0.480 mmol) in toluene (5 mL) at –78 °C. Upon addition, the mixture became translucent white in colour. The mixture was slowly warmed to room temperature and stirred for an additional hour at room temperature before removal of volatiles *in vacuo*. Pentane (5 mL) was added to the crude residue, and the mixture was centrifuged to remove LiCl. Colourless needle crystals of **8** were obtained upon storing the supernatant at –30 °C (242 mg, 45%). ^{1}H NMR (C$_6$D$_6$, 600 MHz, 298 K): δ 3.32 (m, 8H, CH$_2$C*H*$_2$O), 2.41 (m, 6H, N(C*H*$_3$)$_2$), 1.24 (m, 8H, C*H*$_2$CH$_2$O), 0.48 (s, 27H, Ge(C*H*$_3$)$_3$) ppm. ^{13}C{^{1}H} NMR (C$_6$D$_6$, 151 MHz, 298 K): δ 68.21 (s, CH$_2$*C*H$_2$O), 47.91 (s, N(*C*H$_3$)$_2$), 25.43 (s, *C*H$_2$CH$_2$O), 4.04 (s, Ge(*C*H$_3$)$_3$) ppm. ^{11}B{^{1}H} NMR (C$_6$D$_6$, 193 MHz, 298 K): δ –13.25 (s) ppm. **C$_{19}$H$_{49}$NO$_2$BGe$_3$Li (559.25 g·mol^{-1}):** calcd. C 40.81, H 8.83, N 2.50%; found. C 40.46, H 9.09, N 2.69%.

(Me$_3$Ge)$_2$B(TMP) (9). A solution of B(TMP)Cl$_2$ (752.0 mg, 3.388 mmol) in toluene (5 mL) was added dropwise via syringe to a stirred solution of {Me$_3$GeLi(THF)$_2$}$_2$ (**3**; 1.822 g, 3.388 mmol) in toluene (10 mL) at –78 °C. Upon addition, the mixture became translucent white in colour. The mixture was slowly warmed to room temperature and stirred overnight before removal of volatiles *in vacuo*. 5 mL of toluene was added to the crude residue and the mixture was centrifuged to remove LiCl. Upon removal of the solvent *in vacuo*, compound **9** was obtained as stark white solid (1.2231 g, 94%). Colourless needle crystals of **9** were obtained by crystallization from pentane at –30 °C. ^{1}H NMR (C$_6$D$_6$, 600 MHz, 298 K): δ 1.42-1.51 (m, 6H, C*H*$_2$C*H*$_2$), 1.28 (s, 12H, C(C*H*$_3$)$_2$), 0.51 (s, 18H, Ge(C*H*$_3$)$_3$) ppm. ^{13}C{^{1}H} NMR (C$_6$D$_6$, 161 MHz, 298 K): δ 58.74 (s, *C*(CH$_3$)$_2$), 35.62 (s, 3,5-CH$_2$), 33.49 (s, C(*C*H$_3$)$_2$), 14.47 (s, 4-*C*H$_2$), 4.37 (s, Ge(*C*H$_3$)$_3$) ppm. ^{11}B{^{1}H} NMR (C$_6$D$_6$, 193 MHz, 298 K): δ 63.52 (s) ppm. **C$_{15}$H$_{36}$NBGe$_2$ (386.53 g·mol^{-1}):** calcd. C 46.61, H 9.39, N 3.62%; found. C 46.26, H 9.48, N 3.43%.

ASSOCIATED CONTENT

Supporting Information

Supporting Information (crystallographic data, NMR spectra, summary tables, X-ray diffractogram) (PDF).

AUTHOR INFORMATION

Corresponding Author

* D.J.H.E.: tel, 905-525-9140 x23307; fax, 905-522-2509; e-mail, emslied@mcmaster.ca.

ACKNOWLEDGMENT

D.J.H.E. thanks NSERC of Canada for a Discovery Grant, Intel Corporation for funding support via the Semiconductor Research Corporation, and the Ontario government for an Ontario Research Fund Research Excellence (ORF-RE) grant. M.A.H. thanks NSERC of Canada for PGS-D award. We are grateful to Dr. Jeffrey S. Price from the Emslie Lab for his assistance with X-ray crystallography.

NOTES AND REFERENCES

¶ The fate of the extruded "GeMe$_2$" remains unknown.

† Literature values of reaction byproduct NMR chemical shifts were used where available, and references are provided in Table S3. In other cases, spectra were obtained in this work (Figure S35).

‡ Heating the precipitate at 100 °C for 24 hours under dynamic vacuum afforded a white powder that was insoluble in THF, with a powder X-ray diffractogram (Figure S48) that does not match any material in the International Centre for Diffraction Database.

§ Attempts to deliver compound **7** at 85 °C were unsuccessful due to insufficient volatility, and maintaining the bubbler at 95 °C led to complete decomposition after several days.

(1) Shivakumar, D. T.; Knežević, T.; Nanver, L. K. Nanometer-thin pure boron CVD layers as material barrier to Au or Cu metallization of Si. *J. Mater. Sci. Mater. Electron.* **2021**, *32*, 7123-7135.
(2) Qi, L.; Mok, K. R. C.; Aminian, M.; Charbon, E.; Nanver, L. K. UV-Sensitive Low Dark-Count PureB Single-Photon Avalanche Diode. *IEEE Transactions on Electron Devices* **2014**, *61*, 3768-3774.
(3) Mohammadi, V.; Qi, L.; Golshani, N.; Mok, C. K. R.; de Boer, W. B.; Sammak, A.; Derakhshandeh, J.; van der Cingel, J.; Nanver, L. K. VUV/Low-Energy Electron Si Photodiodes With Postmetal 400 °C PureB Deposition. *IEEE Electron Device Letters* **2013**, *34*, 1545-1547.
(4) Qi, L.; Sluyterman, S.; Kooijman, K.; Mok, K. R.; Nanver, L. K. PureB single-photon avalanche diodes for low-energy electron detection down to 200 eV. *Opt. Lett.* **2015**, *40*, 300-303.
(5) Huang, K.-C.; Dahal, R.; LiCausi, N.; Lu, J. J.-Q.; Danon, Y.; Bhat, I. B. Boron filling of high aspect ratio holes by chemical vapor deposition for solid-state neutron detector applications. *J. Vac. Sci. Technol., B* **2012**, *30*, 051204-051201-051204-051206.
(6) Liu, X.; Nanver, L. K.; Scholtes, T. L. M. Nanometer-Thin Pure Boron Layers as Mask for Silicon Micromachining. *Journal of Microelectromechanical Systems* **2017**, *26*, 1428-1434.
(7) Liu, X.; Italiano, J.; Scott, R.; Nanver, L. K. Silicon micromachining with nanometer-thin boron masking and membrane material. *Mater. Res. Express* **2019**, *6*, 116438.
(8) Mok, K. R. C.; van de Loo, B. W. H.; Vlooswijk, A. H. G.; Kessels, W. M. M.; Nanver, L. K. Boron-Doped Silicon Surfaces From B_2H_6 Passivated by ALD Al_2O_3 for Solar Cells. *IEEE Journal of Photovoltaics* **2015**, *5*, 1310-1318.
(9) Hållstedt, J.; Parent, A.; Östling, M.; Radamson, H. H. Incorporation of boron in SiGe(C) epitaxial layers grown by reduced pressure chemical vapor deposition. *Mater. Sci. Semicond. Process.* **2005**, *8*, 97-101.
(10) Tillack, B.; Ritter, G.; Krüger, D.; Zaumseil, P.; Morgenstern, G.; Glowatzki, K.-D. Sharp boron doping within thin SiGe layer by rapid

thermal chemical vapour deposition. *Mater. Sci. Technol.* **1995**, *11*, 1060-1064.
(11) Tsai, C.-E.; Lu, F.-L.; Chen, P.-S.; Liu, C. W. Boron-doping induced Sn loss in GeSn alloys grown by chemical vapor deposition. *Thin Solid Films* **2018**, *660*, 263-266.
(12) Tsai, C.-E.; Lu, F.-L.; Liu, Y.-C.; Ye, H.-Y.; Liu, C. W. Low Contact Resistivity to Ge Using *In-Situ* B and Sn Incorporation by Chemical Vapor Deposition. *IEEE Transactions on Electron Devices* **2020**, *67*, 5053-5058.
(13) Frauenrath, M.; Concepción, O.; Gauthier, N.; Nolot, E.; Buca, D.; Hartmann, J. M. Advances in In Situ Boron and Phosphorous Doping of SiGeSn. *ECS J. Solid State Sci. Technol.* **2023**, *12*, 064001.
(14) Mekan, O.; Magedov, I. V.; Frolova, L. V.; Chandler, G.; Garcia, J.; Bethke, D.; Shaner, E. A.; Kalugin, N. G. Chemical Vapor Deposition of Phosphorous- and Boron-Doped Graphene Using Phenyl-Containing Molecules. *J. Nanosci. Nanotechnol.* **2015**, *15*, 4883-4886.
(15) Zhai, Z.; Shen, H.; Chen, J.; Li, X.; Li, Y. Metal-Free Synthesis of Boron-Doped Graphene Glass by Hot-Filament Chemical Vapor Deposition for Wave Energy Harvesting. *ACS Appl. Mater. Interfaces* **2020**, *12*, 2805-2815.
(16) Ramamurti, R.; Becker, M.; Schuelke, T.; Grotjohn, T. A.; Reinhard, D. K.; Asmussen, J. Deposition of thick boron-doped homoepitaxial single crystal diamond by microwave plasma chemical vapor deposition. *Diamond Relat. Mater.* **2009**, *18*, 704-706.
(17) Lü, J. W.; Feng, Y. J.; Peng, H. Y.; Chen, Y. Q. Influence of Boron Doping on Growth Characteristic of Diamond Films Prepared by Hot Cathode DC Chemical Vapor Deposition. *J. Inorg. Mater.* **2009**, *24*, 607-611.
(18) Teraji, T.; Isoya, J.; Watanabe, K.; Koizumi, S.; Koide, Y. Homoepitaxial diamond chemical vapor deposition for ultra-light doping. *Mater. Sci. Semicond. Process.* **2017**, *70*, 197-202.
(19) Mazaheri, A.; Javadi, M.; Abdi, Y. Chemical Vapor Deposition of Two-Dimensional Boron Sheets by Thermal Decomposition of Diborane. *ACS Appl. Mater. Interfaces* **2021**, *13*, 8844-8850.
(20) Kaneti, Y. V.; Benu, D. P.; Xu, X.; Yuliarto, B.; Yamauchi, Y.; Golberg, D. Borophene: Two-dimensional Boron Monolayer: Synthesis, Properties, and Potential Applications. *Chem. Rev.* **2022**, *122*, 1000-1051.
(21) Thammaiah, S. D.; Liu, X.; Knežević, T.; Batenburg, K. M.; Aarnink, A. A. I.; Nanver, L. K. PureB diode fabrication using physical or chemical vapor deposition methods for increased back-end-of-line accessibility. *Solid-State Electron.* **2021**, *177*, 107938.
(22) Mohammadi, V.; de Boer, W. B.; Nanver, L. K. Temperature dependence of chemical-vapor deposition of pure boron layers from diborane. *Appl. Phys. Lett.* **2012**, *101*, 111906.
(23) Sezgi, N. A.; Dogu, T.; Ozbelge, H. O. Mechanism of CVD of boron by hydrogen reduction of BCl_3 in a dual impinging-jet reactor. *Chem. Eng. Sci.* **1999**, *54*, 3297-3304.
(24) Emslie, D. J. H.; Chadha, P.; Price, J. S. Metal ALD and pulsed CVD: Fundamental reactions and links with solution chemistry. *Coord. Chem. Rev.* **2013**, *257*, 3282-3296.
(25) For thermal ALD of main group elements, see: (a) Pore, V.; Knapas, K.; Hatanpää, T.; Sarnet, T.; Kemell, M.; Ritala, M.; Leskelä, M.; Mizohata, K. Atomic Layer Deposition of Antimony and its Compounds Using Dechlorosilylation Reactions of Tris(triethylsilyl)antimony. *Chem. Mater.* **2011**, *23*, 247-254. (b) Blakeney, K. J.; Winter, C. H. Atomic Layer Deposition of Aluminum Metal Films Using a Thermally Stable Aluminum Hydride Reducing Agent. *Chem. Mater.* **2018**, *30*, 1844-1848. (c) Stevens, E. C.; Mousa, M. B. M.; Parsons, G. N. Thermal Atomic Layer Deposition of Sn Metal using a Vapor Phase Silyl Dihydropyrazine Reducing Agent. *J. Vac. Sci. Technol., A* **2018**, *36*, 06A106. (d) Cheng, L.; Adinolfi, V.; Weeks, S. L.; Barabash, S. V.; Littau, K. A. Conformal deposition of GeTe films with tunable Te composition by atomic layer deposition. *J. Vac. Sci. Technol., A* **2019**, *37*, 020907. (e) Al Hareri, M.; Emslie, D. J. H. Room-Termperature Atomic Layer Deposition of Elemental Antimony. *Chem. Mater.* **2022**, *34*, 2400-2409. (f) Kim, C.; Hur, N.; Yang, J.; Oh, S.; Yeo, J.; Jeong, H. Y.; Shong, B.; Suh, J. Atomic Layer Deposition Route to Scalable, Electronic-Grade van der Waals Te Thin Films. *ACS Nano* **2023**, *17*, 15776-15786.
(26) Attempted boron ALD using B_2F_4 and Si_2H_6 did not yield films of appreciable thickness: Mane, A. U.; Elam, J. W.; Goldberg, A.; Seidel, T. E.; Halls, M. D.; Current, M. I.; Despres, J.; Byl, O.; Tang, Y.; Sweeney, J. *J. Vac. Sci. Technol., A* **2016**, *34*, 01A132.
(27) Biffar, W.; Nöth, H.; Pommerening, H. Stabilization of Diborane(4) Derivatives by *tert*-Butyl Groups: The First Tetraalkyldiborane(4). *Angew. Chem. Int. Ed.* **1980**, *19*, 56-57.
(28) Herberhold, M.; Dörfler, U.; Wrackmeyer, B. Dynamic Behaviour of Some Boryl-Substituted Ferrocenes. *Polyhedron* **1995**, *14*, 2683-2689.
(29) Herberich, G. E.; Englert, U.; Ganter, B.; Pons, M.; Wang, R. Borabenzene Derivatives. 28. Pinene-Fused Dihydroborinines, Boratabenzenes, and a Borabenzene-Pyridine Adduct. *Organometallics* **1999**, *18*, 3406-3413.
(30) Herberich, G. E.; Englert, U.; Fischer, A.; Ni, J.; Schmitz, A. Borabenzene Derivatives. 29. Synthesis and Structural Diversity of Bis(boratabenzene)scandium Complexes. Structures of $[ScCl(C_5H_5BMe)_2]_2$, $[ScCl(3,5\text{-}Me_2C_5H_3BNMe_2)_2]_2$, and $ScCl[3,5\text{-}Me_2C_5H_3BN(SiMe_3)_2]_2$. *Organometallics* **1999**, *18*, 5496-5501.
(31) Braunschweig, H.; Colling, M.; Kollann, C.; Englert, U. The first silyl- and germylboryl complexes: synthesis from novel (dichloro)silyl- and (dichloro)germylboranes, structure and reactivity. *J. Chem. Soc., Dalton Trans.* **2002**, 2289-2296.
(32) Emslie, D. J. H.; Piers, W. E.; Parvez, M. 2,2'-Diborabiphenyl: A Lewis Acid Analogue of 2,2'-Bipyridine. *Angew. Chem. Int. Ed.* **2003**, *42*, 1252-1255.
(33) Jaska, C. A.; Emslie, D. J. H.; Bosdet, M. J. D.; Piers, W. E.; Sorensen, T. S.; Parvez, M. Triphenylene Analogues with $B_2N_2C_2$ Cores: Synthesis, Structure, Redox Behavior, and Photophysical Properties. *J. Am. Chem. Soc.* **2006**, *128*, 10885-10896.
(34) Rodriguez, A.; Fuks, G.; Bourg, J.-B.; Bourissou, D.; Thama, F. S.; Bertrand, G. 1,3-Diborata-2,4-diphosphoniocyclobutane-1,3-diyls communicate through a para-phenylene linker. *Dalton Trans* **2008**, 4482-4487.
(35) Ota, K.; Kinjo, R. A Neutral and Aromatic Boron-Rich Inorganic Benzene. *Angew. Chem. Int. Ed.* **2020**, *59*, 6572-6575.
(36) Moezzi, A.; Olmstead, M. M.; Power, P. P. The Structure of 1,2-Diaryl-1,2-bis(dimethylamino)diboron Compounds and Related Species: Boron-Nitrogen Analogues of Buta-1,3-dienes. *J. Chem. Soc. Dalton Trans.* **1992**, 2429-2434.
(37) Ali, H. A.; Goldberg, I.; Srebnik, M. Tetra(pyrrolidino)diborane(4), $[(C_4H_8N)_2B]_2$, as a New Improved Alternative Synthetic Route to Bis(pinacolato)diborane(4) - Crystal Structures of the Intermediates. *Eur. J. Inorg. Chem.* **2002**, 73-78.
(38) Rodriguez, A.; Tham, F. S.; Schoeller, W. W.; Bertrand, G. Catenation of two singlet diradicals: synthesis of a stable tetraradical (tetraradicaloid). *Angew. Chem. Int. Ed.* **2004**, *43*, 4876-4880.
(39) Janes, T.; Diskin-Posner, Y.; Milstein, D. Synthesis and Reactivity of Cationic Boron Complexes Distorted by Pyridine-based Pincer Ligands: Isolation of a Photochemical Hofmann-Martius-type Intermediate. *Angew. Chem. Int. Ed.* **2020**, *59*, 4932-4936.
(40) Thiess, T.; Ernst, M.; Kupfer, T.; Braunschweig, H. Facile Access to Substituted 1,4-Diaza-2,3-Diborinines. *Chem. Eur. J.* **2020**, *26*, 2967-2972.
(41) Al Hareri, M.; Emslie, D. J. H. Room-Temperature Atomic Layer Deposition of Elemental Antimony. *Chem. Mater.* **2022**, *34*, 2400-2409.
(42) Pore, V.; Knapas, K.; Hatanpää, T.; Sarnet, T.; Kemell, M.; Ritala, M.; Leskelä, M.; Mizohata, K. Atomic Layer Deposition of Antimony and its Compounds Using Dechlorosilylation Reactions of Tris(triethylsilyl)antimony. *Chem. Mater.* **2011**, *23*, 247-254.
(43) Pore, V.; Hatanää, T.; Ritala, M.; Leskelä, M. Atomic Layer Deposition of Metal Tellurides and Selenides Using Alkylsilyl Compounds of Tellurium and Selenium. *J. Am. Chem. Soc.* **2009**, *131*, 3478-3480.
(44) Charvot, J.; Zazpe, R.; Macak, J. M.; Bureš, F. Organoselenium Precursors for Atomic Layer Deposition. *ACS Omega* **2021**, *6*, 6554-6558.
(45) Knapas, K.; Hatanpää, T.; Ritala, M.; Leskelä, M. In Situ Reaction Mechanism Studies on Atomic Layer Deposition of Sb_2Te_3 and GeTe from $(Et_3Si)_2Te$ and Chlorides. *Chem. Mater.* **2010**, *22*, 1386-1391.

(46) Wiberg, N.; Amelunxen, K.; Blank, T.; Lerner, H.-W.; Polborn, K.; Nöth, H.; Littger, R.; Rackl, M.; Schmidt-Amelunxen, M.; Schwenk-Kircher, H.; Warchold, M. Supersilyltrielanes R*$_n$EHal$_{3-n}$ (E = Triel, R* = Si*t*Bu$_3$): Syntheses, Characterization, Reactions, Structures. *Z. Naturforsch. B* **2001**, *56*, 634-651.
(47) Han, B.; Kim, Y.-J.; Park, J.-M.; Yusup, L. L.; Shin, J.; Lee, W.-J. Reaction Mechanism for Atomic Layer Deposition of Germanium Ditelluride Thin Films. *J. Nanosci. Nanotechnol.* **2017**, *17*, 3472-3476.
(48) Vihervaara, A.; Hatanpää, T.; Mizohata, K.; Chundak, M.; Popov, G.; Ritala, M. A low-temperature thermal ALD process for nickel utilizing dichlorobis(triethylphosphine)nickel(II) and 1,4-bis(trimethylgermyl)-1,4-dihydropyrazine. *Dalton Trans.* **2022**, *51*, 10898-10908.
(49) Vihervaara, A.; Hatanpää, T.; Nieminen, H. E.; Mizohata, K.; Chundak, M.; Ritala, M. Reductive Thermal Atomic Layer Deposition Process for Gold. *ACS Mater. Au* **2023**, *3*, 206-214.
(50) Nöth, H.; Höllerer, G. Organylsilyl-borane. *Chem. Ber.* **1966**, *99*, 2197-2205.
(51) Nöth, H., Metalloboranes. In *Science of Synthesis*, Thieme: 2005; Vol. 6, pp 139-178.
(52) Biffar, W.; Nöth, H.; Schwerthöffer, R. Synthesis and Reactivity of Trimethylsilylboranes. *Liebigs Ann. Chem.* **1981**, 2067-2080.
(53) Still, W. C. Conjugate Addition of Trimethysilyllithium. A Preparation of 3-Silyl Ketones. *J. Org. Chem.* **1976**, *41*, 3063-3064.
(54) Kamio, S.; Imagawa, T.; Nakamoto, M.; Oestreich, M.; Yoshida, H. HMPA-Free Generation of Trialkylsilyllithium Reagents and Its Applications to the Synthesis of Silylboronic Esters. *Synthesis* **2021**, *53*, 4678-4681.
(55) Buynak, J. D.; Geng, B. Synthesis and Reactivity of Silylboranes. *Organometallics* **1995**, *14*, 3112-3115.
(56) Habereder, T.; Nöth, H. Synthesis and Structures of Amino(triphenylgermyl) Boranes and Trihydro(triphenylgermyl) Borates. *Z. Anorg. Allg. Chem.* **2001**, *627*, 1003-1012.
(57) Biffar, W.; Nöth, H. Tris(trimethylsilyl)silyl Boranes and Tris(trimethylsilyl)silyl Borates. *Z. Naturforsch. B* **1981**, *36*, 1509-1515.
(58) Hengge, E.; Wolfer, D. Boracyclopentasilan, ein neuer Typ heterocyclischer Silane. *Angew. Chem.* **1973**, *7*, 304.
(59) Markov, J.; Fischer, R.; Wagner, H.; Noormofidi, N.; Baumgartner, J.; Marschner, C. Open, cyclic, and bicyclic compounds of double silylated phosphorus and boron. *Dalton Trans.* **2004**, 2166-2169.
(60) Purkait, T. K.; Press, E. M.; Marro, E. A.; Siegler, M. A.; Klausen, R. S. Low-Energy Electronic Transition in SiB Rings. *Organometallics* **2019**, *38*, 1688-1698.
(61) Heine, A.; Herbst-lrmer, R.; Sheldrick, G. M.; Stalke, D. Structural Characterization of Two Modifications of Tris(tetrahydrofuran)(tris(trimethylsilyI)silyl)lithium: A Compound with a ^{29}Si-^{7}Li NMR Coupling. *Inorg. Chem.* **1993**, *32*, 2694-2698.
(62) Wiberg, N.; Amelunxen, K.; Lemer, H.-W.; Schuster, H.; Nöth, H.; Krossing, I.; Schmidt-Amelunxen, M.; Seifert, T. Donorfreie und donorhaltige Supersilylalkalimetalle ^{t}Bu$_3$SiM: Synthesen, Charakterisierung, Strukturen. *J. Organomet. Chem.* **1997**, *542*, 1-18.
(63) Piers, E.; Lemieux, R. Reaction of (Trimethylgermyl)copper(I)-Dimethyl Sulfide with Acyl Chlorides: Efficient Syntheses of Functionalized Acyltrimethylgermanes. *Organometallics* **1995**, *14*, 5011-5012.
(64) Schumann, H.; Nickel, S.; Loebel, J.; Pickardt, J. Organometallic Compounds of the Lanthanides. 42. Bis(dimethoxyethane)lithium bis(cyclopentadienyl)bis(trimethylsilyl)lanthanide Complexes. *Organometallics* **1988**, *7*, 2004-2009.
(65) Iwamoto, T.; Okita, J.; Kabuto, C.; Kira, M. Sila-metalation Route to Hydrido(trialkylsilyl)silyllithiums. *J. Am. Chem. Soc.* **2002**, *124*, 11604-11605.
(66) Nanjo, M.; Maehara, M.; Ushida, Y.; Awamura, Y.; Mochida, K. Convenient access to optically active silyl- and germyllithiums: synthesis, absolute structure, and reactivity. *Tetrahedron Lett.* **2005**, *46*, 8945-8947.
(67) Mochida, K.; Ogawa, S.; Naito, N.; Gaber, A. E.-A.; Usui, Y.; Nanjo, M. Preparation, Structural Characterization, and Reactivities of (Digermanyl)lithium. Its Application to the Synthesis of Bis(1,1-diphenyl-2,2,2-trimethyldigermanyl)platinum(II). *Chem. Lett.* **2007**, *36*, 414-415.
(68) Freitag, S.; Herbst-Irmer, R.; Lameyer, L.; Stalke, D. Observation of a Ge-Li Bond: Donor-Base-Stabilized (Tris(trimethylsilyl)germyl)lithium. *Organometallics* **1996**, *15*, 2839-2841.
(69) Nanjo, M.; Nanjo, E.; Mochida, K. Tris(trimethylsilyl)-Substituted Heavy Group 14-Element-Centered Anions: Unsolvated Trimeric Germyllithium and Solvated Dimeric Silyl- and Stannyllithiums. *Eur. J. Inorg. Chem.* **2004**, 2961-2967.
(70) Habereder, T.; Nöth, H.; Suter, M. Synthesis, Structure and Bonding in Triorganogermyl-alanes and Triphenylgermyl-aluminates. *Z. Naturforsch. B* **2009**, *64*, 1387.
(71) Bond distance range based on a search of the Cambridge Structural Database for silylborane compounds. 100% of the B-Si distances in the CSD fall within the range described. CSD accessed via conquest CSD on May 23, 2024; version 5.42, updated November 2020).
(72) Bond distance range based on a search of the Cambridge Structural Database for silylborane compounds. 85% of the B-N distances in the CSD fall within the range described. CSD accessed via conquest CSD on May 23, 2024; version 5.42, updated November 2020).
(73) Fan, M.; Paine, R. T.; Duesler, E. N.; Nöth, H. Synthesis and Molecular Structure of Tris[(trimethylsilyl)silyl](diisopropylamino)(diphenylphosphino)borane. *Z. Anorg. Allg. Chem.* **2006**, *632*, 2443-2446.
(74) Haasea, M.; Klingebiel, U.; Boese, R.; Polk, M. Stabilisierung und Reaktionen von Iminoboranen Kristallstruktur von (*tert*-Butylimino)tris(trimethylsilyl)silyl]boran. *Chem. Ber.* **1986**, *119*, 1117-1126.
(75) Lattice Energies. In *CRC Handbook of Chemistry and Physics*, 103 ed.; J. R. Rumble, Ed. Taylor & Francis Group: 2022-2023.
(76) Biffar, W.; Nöth, H. (Trimethylsilyl)borates from Alkoxyboranes and Trimethylsilyllithium. *Chem. Ber.* **1982**, *115*, 934-945.
(77) Lippert, W.; Nöth, H.; Ponikwar, W.; Seifert, T. Preparation and Structural Characterization of Lithium Silylborates. *Eur. J. Inorg. Chem.* **1999**, 817-823.
(78) Lubitz, K.; Sharma, V.; Shukla, S.; Berthel, J. H. J.; Schneider, H.; Hoßbach, C.; Radius, U. Asymmetrically Substituted Tetrahedral Cobalt NHC Complexes and Their Use as ALD as well as Low-Temperature CVD Precursors. *Organometallics* **2018**, *37*, 1181-1191.
(79) Baunemann, A.; Lemberger, M.; Bauer, A. J.; Parala, H.; Fischer, R. A. MOCVD of TaN Using the All-Nitrogen-Coordinated Precursors [Ta(NEtMe)$_3$(N-^{t}Bu)], [Ta(NEtMe)(N-^{t}Bu){C(N-^{i}Pr)$_2$(NEtMe)}$_2$], and [Ta(NMeEt)$_2$(N-^{t}Bu){Me$_2$N-N(SiMe$_3$)}]. *Chem. Vap. Deposition* **2007**, *13*, 77-83.
(80) Gilman, H.; Smith, C. L. Tetrakis(trimethylsilyl)silane. *J. Organomet. Chem.* **1967**, *8*, 245-253.
(81) Weidenbruch, M.; Pesel, H.; Peter, W.; Steichen, R. Silicium-Verbindungen Mit Starken Intramolekularen Sterischen Wechselwirkungen. VI. Darstellung Und Eigenschaften Des Tri-t-butylsilans Und Der Tri-t-butylhalogensilane. *J. Organomet. Chem.* **1977**, *141*, 9-21.
(82) Nöth, H.; Weber, S. A Convenient Synthesis of an Amino-Imino-Borane and its Adducts with Boron Trichloride and Boron Tribromide. *Z. Naturforsch. B* **1983**, *38*, 1460-1465.
(83) Banister, A. J.; Greenwood, N. N.; Straughan, B. P.; Walker, J. Monomeric Dimethylaminoboron Dihalides. *J. Chem. Soc.* **1964**, 995-1000.
(84) Harris, R. K.; Becker, E. D.; Menezes, S. M. C. d.; Goodfellow, R.; Granger, P. NMR Nomenclature. Nuclear Spin Properties and Conventions for Chemical Shifts. *Pure Appl. Chem.* **2001**, *73*, 1795-1818.
(85) Sheldrick, G. M. SHELXT - Integrated space-group and crystal-structure determination. *Acta Crystallogr. Sect. A: Found. Crystallogr.* **2015**, *71*, 3-8.
(86) Sheldrick, G. M. Crystal structure refinement with SHELXL. *Acta Crystallogr. Sect. C: Cryst. Struct. Commun.* **2015**, *71*, 3-8.
(87) Dolomanov, O. V.; Bourhis, L. J.; Gildea, R. J.; Howard, J. A. K.; Puschmann, H. OLEX2: A complete structure solution, refinement and analysis program. *J. Appl. Crystallogr.* **2009**, *42*, 339-341.

Authors are required to submit a graphic entry for the Table of Contents (TOC) that, in conjunction with the manuscript title, should give the reader a representative idea of one of the following: A key structure, reaction, equation, concept, or theorem, etc., that is discussed in the manuscript. Consult the journal's Instructions for Authors for TOC graphic specifications.

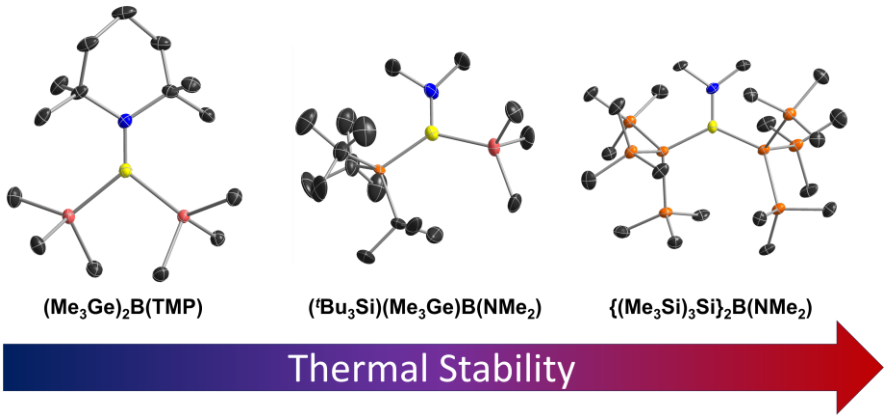

Accompanying text:

Boranes featuring bulky hypersilyl or supersilyl groups, and/or sterically unencumbered trimethylgermyl substituents, were synthesized for investigation as potential precursors for atomic layer deposition (ALD) of boron, and the thermal stability of the compounds was found to correlate strongly with the number of bulky silyl groups.